BULLETIN OF THE POLISH ACADEMY OF SCIENCES
TECHNICAL SCIENCES, Vol. 70(1), 2022, Article number: e139394
DOI: 10.24425/bpasts.2021.139394

Minimizing the number of layers of the quasi-one-dimensional phononic structures

Sebastian GARUS[1]*, **Wojciech SOCHACKI**[1], **Mariusz KUBANEK**[2], **and Marcin NABIAŁEK**[3]

[1] Faculty of Mechanical Engineering and Computer Science, Department of Mechanics and Fundamentals of Machinery Design, Czestochowa University of Technology, Dąbrowskiego 73, 42-201 Czestochowa, Poland
[2] aculty of Mechanical Engineering and Computer Science, Department of Computer Science, Czestochowa University of Technology, Dąbrowskiego 73, 42-201 Czestochowa, Poland
[3] Faculty of Production Engineering and Materials Technology, Department of Physics, Czestochowa University of Technology, Armii Krajowej 19, 42-201 Czestochowa, Poland

Abstract. In the work, multi-criteria optimization of phononic structures was performed to minimize the transmission in the frequency range of acoustic waves, eliminate high transmission peaks with a small half-width inside of the band gap, and what was the most important part of the work – to minimize the number of layers in the structure. Two types of the genetic algorithm were compared in the study. The first one was characterized by a constant number of layers (GACL) of the phononic structure of each individual in each population. Then, the algorithm was run for a different number of layers, as a result of which the structures with the best value of the objective function were determined. In the second version of the algorithm, individuals in populations had a variable number of layers (GAVL) which required a different type of target function and crossover procedure. The transmission for quasi-one-dimensional phononic structures was determined with the use of the transfer matrix method algorithm. Based on the research, it can be concluded that the developed GAVL algorithm with an appropriately selected objective function achieved optimal solutions in a much smaller number of iterations than the GACL algorithm, and the value of the k parameter below 1 leads to faster achievement of the optimal structure.

Key words: mechanical waves; phononic; transfer matrix; bandgap; genetic algorithm.

1. INTRODUCTION

The artificial periodic structure, which is the basis for the structure of phononic crystals (PnC) and phononic structures (PhS), has been the subject of intensive research in recent years [1–9]. This structure has specific properties related to the propagation of acoustic and elastic waves in it. One of these properties is the existence of the so-called band gap (BG) which does not allow the elastic waves of a specified frequency range to pass through the phononic crystal. Both the BG width and the center frequency depend on the type of material and the geometric parameters of the PnC and can be controlled. To control the BG, much work has been done to optimize the topology of the PnCs [10–20]. A way to optimize the topology of the design of materials and structures with gaps is presented in the extensive work by Bendsøe and Sigmund [10]. Siegmund and Jensen [11] and Xie *et al.* [12], using the topology optimization method, designed a PnC with "pure bands" for a specific frequency range. PnC topology optimization in many studies is carried out with the use of genetic algorithms (GA). Using the plane wave expansion method, Zhong *et al.* [13] using GA maximized the bandgap width in PnC. Using similar methods, Liu *et al.* [14] optimized PnC topology with square lattices. The authors used the two-stage GA in conjunction with the fast plane wave expansion method. The two-way optimization method inspired by the evolutionary penalization parameter was carried out by Huang and Xie in [15]. Optimal solutions were obtained for structures consisting of both single and multiple materials. Dong *et al.* [16] optimized the PnC topology using the reverse scheme of the two-stage GA. The authors were given the maximum BG between adjacent two-dimensional bands. Li *et al.* [17] applied a bidirectional genetic optimization algorithm to obtain the maximum bandwidth between two adjacent bands in a square unit cell. Gazonas *et al.* [18] described the use of GA to optimally design phononic bands in periodic biphasic elastic structures. In the work [19] Hussein *et al.* used a multi-body GA to design the topology of one-dimensional periodic PnC unit cells. Optimal topologies that produce large BG shifts in one- and two-dimensional nonlinear phononic crystals are presented by Manktelow *et al.* at work [20]. The article discusses the issue of optimal PnC topology design. For this purpose, a GA was used, which allows us to obtain optimal distributions of individual elements of the PnC network. Optimum distribution

*e-mail: gari.sg@gmail.com

Manuscript submitted 2021-04-02, revised 2021-08-25, initially accepted for publication 2021-08-26, published in February 2022.

is understood as ensuring maximum BGs under given conditions. The article [21] by Hedayatras *et al*. presented a polyoptimization of phononic plate topology with experimental validation to investigate the relationship between a BG efficiency and the effective bending stiffness of the plate. Research aimed at increasing the total BG was carried out by L. Chen *et al*. in [22] by performing a BG optimization for chiral PnCs. Han and Hang in [23] applied a GA with the method of plane wave expansion to optimize a three-phase PnC for a larger relative BG. In their article [24] Garus and Sochacki solved the problem of the optimal design of a PnC topology as an acoustic filter made of transparent materials. In the paper [25] Chen *et al*. have developed a new topology optimization algorithm of PnCs for unidirectional acoustic transmission based on the bi-directional evolutionary structural optimization (BESO) method. The authors of [26] Han and Zhang used a GA to optimize the topology of a thin PnC plate composed of aluminum and epoxy resin. The genetic algorithm, due to its universality, is also used in other applications, such as [27], in which Chruszczyk presented the process of searching for the peak-to-peak value of the minimum value of a multi-tone signal and in the work [28] by Beniyel *et al*., who optimized the consumption of the selected magnesium alloy. The genetic algorithm was used by the authors to determine the properties of the alloy resulting in its minimal wear and low friction coefficient.

The TMM method is a matrix formalism known and successfully used in many fields of physics. The frequent use of this method in photonics or phononics results from the possibilities it gives concerning the speed of calculations. In the case of an acoustic wave passing through a material layer, the TMM method combines the sound pressure and wave velocities at the entrance and after passing the structure. Therefore, this method facilitates the prediction of transmission and reflection coefficients also in multilayer structures. An interesting work on the general approach to the determination of the mentioned transmission and reflection coefficients is the work of Dazel *et al*. [29]. The TMM method was used by Garus *et al*. in the work [30] for the analysis of three types of multilayer structures with a piezoelectric layer as a defect of the examined structures. Similarly, the TMM method was used by Sigalas and Soukoulis in [31]. The authors analyzed the propagation of elastic waves in multilayer, disordered two-material structures. The TMM method was also used in the work of Luan and Ye [32] to study and analyze the propagation of acoustic waves in a water channel in which many blocks filled with air were placed. In the work of Pop and Cretu [33], the formalism of the split quaternion is presented as equivalent to the TMM formalism for the passage of a wave through a one-dimensional structure with many layers.

In this work, the two genetic algorithms (GA) are compared to minimize at the same time the thickness and transmission of the phononic structures. As part of the algorithm work, structures are designed in which there is no periodicity of the basic cell, i.e. they cannot be classified as phononic crystals (PhC), but the phenomenon of phononic band gap (PhBG) occurs and therefore they are referred to as phononic structures (PhS). The transfer matrix method (TMM) method was used to analyze the wave transition through the examined structures because it facilitates the analysis of unordered structures.

2. MATERIALS AND METHODS

2.1. Transfer matrix method

Figure 1 shows the propagation of the mechanical wave through the multilayer structure, which can be described by the equation

$$\begin{bmatrix} P(f)^{+}_{\text{in}} \\ P(f)^{-}_{\text{in}} \end{bmatrix} = M \begin{bmatrix} P(f)^{+}_{\text{out}} \\ P(f)^{-}_{\text{out}} \end{bmatrix}, \tag{1}$$

where $P(f)^{+}_{\text{in}}$ is the pressure of the mechanical wave incident perpendicularly on the multilayer structure; $P(f)^{-}_{\text{in}}$ is the pressure of the mechanical wave reflected from the structure; $P(f)^{+}_{\text{in}}$ is the pressure of the mechanical wave coming out of the structure; $P(f)^{-}_{\text{out}}$ is always zero. The pressure values are determined for a given frequency f. The signs in the superscript correspond to the wave propagation direction (it was assumed that $+$ corresponds to the right direction in Fig. 1, and $-$ to the left direction).

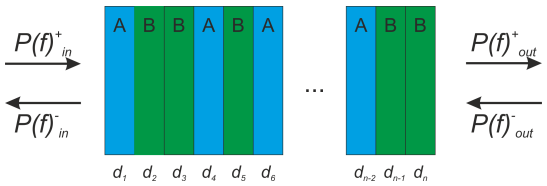

Fig. 1. A quasi one-dimensional phononic structure made of n layers of materials A and B where a given i-th layer has a thickness d_i

The characteristic matrix M of the TMM model for the superlattice structure can be described by

$$M = T_{1,i} \left(\prod_{i=1}^{n-1} R_i T_{i,i+1} \right) R_n T_{n,\text{out}} \,. \tag{2}$$

The mechanical wave propagation in layer i is described by the propagation matrix R_i, which is defined as

$$R_i = \begin{bmatrix} e^{2\pi i f d_i c_i^{-1}} & 0 \\ 0 & e^{-2\pi i f d_i c_i^{-1}} \end{bmatrix}, \tag{3}$$

where d_i is the thickness of layer i and c_i is the phase velocity of the mechanic wave. The transfer matrix $T_{i,i+1}$ between layers i and $i+1$ is described as

$$T_{i,i+1} = \frac{1}{2Z_i} \begin{bmatrix} Z_i + Z_{i+1} & Z_i - Z_{i+1} \\ Z_i - Z_{i+1} & Z_i + Z_{i+1} \end{bmatrix}, \tag{4}$$

where Z_i is the i-layer acoustic impedance which is defined as $Z_i = \rho_i c_i$; ρ_i – i-layer mass density.

$$T(f) = |M_{11}(f)|^{-2} \,. \tag{5}$$

The transmission T for a given frequency f is determined from equation (5) and is influenced by the distribution of the material of the multilayer structure that is contained in the characteristic matrix M.

2.2. Genetic algorithms

Two different solutions using a genetic algorithm are compared in the work. In the first approach, the constant length of the structure in the full cycle of the analyzed population is used (GACL), and then the entire process for different lengths of structures (chromosomes or individuals in GA vocabulary) is repeated. In the second analyzed type of genetic algorithm, variable length of the structure (GAVL) was used. This influenced changes in the objective function and the algorithm for generating a new population from the previous one. It should also be noted that as the number of layers increases, the space of possible solutions increases significantly, as shown in Fig. 2. The genotype in the presented solution is a single structure built of individual genes describing the type of material used in the layer (A or B), while the phenotype is the distribution of transmission values depending on the frequency determined for a given chromosome based on the TMM algorithm from equation (5).

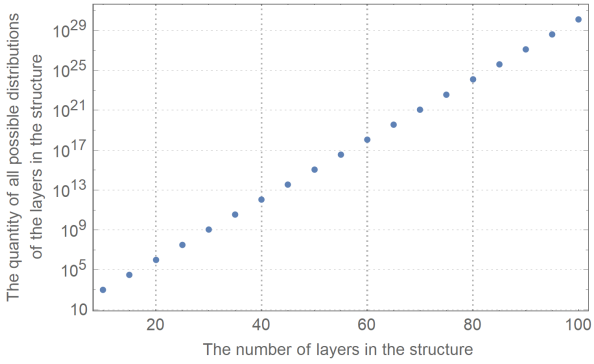

Fig. 2. Influence of the increase in the number of layers in a structure on the size of the searched solution space

The first stage of the genetic algorithms (Fig. 3) is the initialization of the constants controlling the operation of the algorithm and the number of layers in the structure is determined for GACL. The next step is to randomly generate the first population. Then, the transmission for each structure in the population is determined using the TMM algorithm based on equation (5). For each individual of the population, the value of the objective function was calculated, which for GACL is defined as

$$F_{\mathrm{GACL}} = \|F_I\| \, \|F_{DI}\| \tag{6}$$

and for GAVL is given as

$$F_{\mathrm{GAVL}} = F_{\mathrm{GACL}} k + \frac{n - n_{\min}}{n_{\max} - n_{\min}} (1 - kt). \tag{7}$$

The k parameter determines the extent to which the objective function of the GAVL algorithm is influenced by the function defined by equation (6), and by the number of layers of the ana-

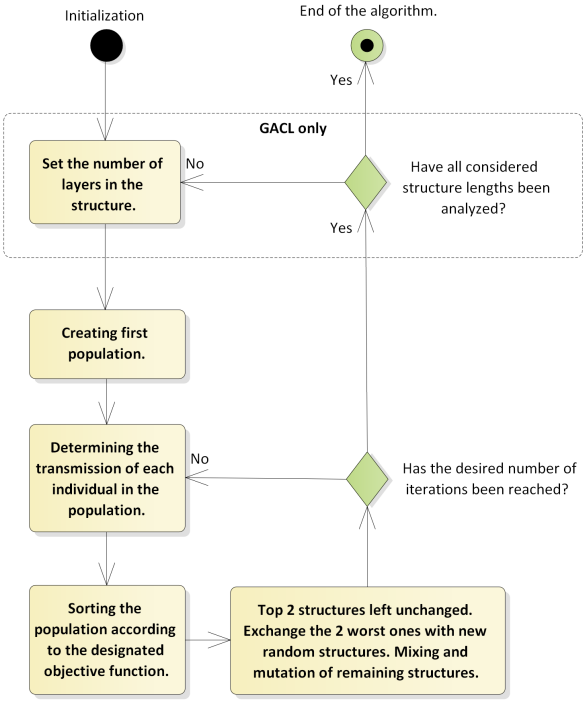

Fig. 3. Activity diagram for optimization algorithms

lyzed structure. The values of the k parameter range from 0 to 1. For the values of the k parameter closer to zero, the structures with the smallest number of layers from the analyzed population are most preferred, and the reduction of transmission and elimination of transmission peaks takes place at a later stage of the algorithm's work. When the values of the k coefficient are closer to 1, it is more important to minimize the transmission and eliminate high transmission peaks with a small half-width, and then in further steps of the algorithm, the most favorable structures in the population are replaced by equivalents characterized by a smaller number of layers. The number of layers n in the structure ranges from $n_{\min}$ to $n_{\max}$.

Because the values of the F_I and F_{DI} functions differ significantly, their normalization was applied, where the minimum was taken as zero, and the highest value of a given component of the objective function was equal to the value of 1. This means that in each population the highest value of the given objective function component is different. This procedure makes it possible to compare the structures only within a given population. To compare the structures between populations, use the function without normalization shown as

$$F_c' = F_I \cdot F_{DI}\,. \tag{8}$$

The components of the objective function F_{GACL} are two normalized subfunctions. The first F_I is responsible for minimizing the transmission $T(f)$ integral in the frequency range from $f_{\min}$ to $f_{\max}$ and is defined as

$$F_I = \int_{f_{\min}}^{f_{\max}} T(f)\,\mathrm{d}f, \tag{9}$$

$$F_I \approx \frac{f_{\max} - f_{\min}}{2h} \sum_{i=1}^{n} \left[T(f_i) + T(f_{i+1}) \right]. \tag{10}$$

The second sub-function F_{DI} of the objective function F_{GACL} is responsible for minimizing the occurrence of narrow high transmission peaks and is given as

$$F_{\mathrm{DI}} = \int_{f_{\min}}^{f_{\max}} F_D(f)\,\mathrm{d}f, \tag{11}$$

where $F_D(f)$ is defined by

$$F_D(f) = \left| \frac{\partial T(f)}{\partial f} \right| \approx \left| \frac{h\left[T\left(f + \frac{f_{\max} - f_{\min}}{n} \right) - T(f) \right]}{f_{\max} - f_{\min}} \right|, \tag{12}$$

considering the above, a numerical approximation of F_{DI} was obtained

$$F_{\mathrm{DI}} \approx \frac{f_{\max} - f_{\min}}{2h} \sum_{i=1}^{n} \left[F_D(f_i) + F_D(f_{i+1}) \right]. \tag{13}$$

The parameter h describes the accuracy of numerical calculations and was set as $h = 8 \cdot 10^4$, which gave a frequency resolution of $\Delta f = 0.25$ Hz.

The transmission fill factor is defined as

$$F_T = \frac{F_I}{f_{\max} - f_{\min}}. \tag{14}$$

Then, in the population group sorted by the objective function appropriate for the algorithm used, the two best structures are left, the two weakest ones are rejected, and the remaining ones are crossed over with the probability resulting from the value of the objective function.

The algorithm was used to select individuals for a crossover of the proportional method of the so-called roulette wheel selection, the angular sectors of which are proportional to the values of the individual objective function. Better adapted individuals are proportionally larger angular sectors on the roulette wheel (greater chance of introducing more descendants to the next generation of the population). The one-point crossing was used, however, in the GAVL algorithm, the lengths of structure elements were also selected so that their total number was at least $n_{\min}$ and at most $n_{\max}$. To avoid the algorithm remaining in the local minimum of solutions, apart from the exchange of two structures in each population, some layers are also mutated in the analyzed structures with a given probability. The process is repeated until a given number of iterations is achieved.

3. RESEARCH

As part of the work, a genetic algorithm with a variable number of layers in the population (GAVL) was developed in order to simultaneously minimize the number of layers within the range from $n_{\min} = 10$ to $n_{\max} = 100$ layers, minimize mechanical wave transmission in the range of acoustic frequencies and minimize the chance of occurrence and reduce the intensity of high transmission peaks with a small half-width (the more layers in the structure, the more such transmission peaks there are). All the above goals are realized by the developed objective function from equation (7). GAVL was compared with the constant number of layers (GACL) algorithm developed in [24], performed for structures with the number of layers from the above range with a step of 5 layers. The GACL algorithm does not cover the full space of solutions to the problem, even though a total of 3800 iterations are performed. GAVL algorithm performed 500 iterations for each k parameter value.

The structures analyzed in the study were made of glass and polyvinyl chloride (PVC). The material parameters are presented in Table 1.

Table 1

Parameters of the materials used [34, 35]

Material	Symbol	Mass density [kg·m^{-3}]	Phase velocity [m·s^{-1}]
Air		1.21	343
Glass	A	3880	4000
PVC	B	66	913

The materials were selected in such a way that there was a large difference in acoustic impedance between them. Absorption was not considered in the considerations so that the gaps only occur due to the structure. The structure is surrounded by air and mechanical waves are analyzed in the range of acoustic frequencies from $f_{\min} = 0$ kHz to $f_{\max} = 20$ kHz. The single-layer thickness in the simulation was 1 mm. There were 20 structures in each population. The chance of a single-layer mutation was 1%.

Figure 4a shows the graphs of the objective function values for the best structures in a population for a given generation number for each of the considered number of layers in the structure.

The determined structures are collected in Table 2, and the corresponding values of the objective function are presented in Fig. 4b. The lowest objective function value was determined for the structure with one hundred layers, and the next two were ninety-five and seventy-layer structures. There was no relationship between the number of layers in the structure and the value of the objective function in the optimal structures found by the genetic algorithm.

Figure 5a shows the objective function values for the best structures in a population for a given k parameter, and the objective function values for the best structures found using the GAVL algorithm are shown in Fig. 5b. The convergence plots of Figs. 4a and 5a show that the appropriate number of iterations of the algorithm was selected.

Figure 6 shows the transmission for the best-determined structures for each considered number of layers in the structure in the GACL algorithm.

For better readability, the transmission was converted to sound pressure level (SPL) at the sound source with an SPL

Table 2
Distribution of materials in the best structures found for a given number of layers

The number of layers	Best structure
10	A_{10}
15	A_{15}
20	$BA_8B_2A_9$
25	$A_{14}B_2A_7B_2$
30	$A_{15}BAB_2A_4BA_6$
35	$B_3A_{16}B_2AB_2A_{11}$
40	$ABA_{10}B_2A_{25}B$
45	$A_6BABA_4B_2A_2B_2AB_3A_{19}B_3$
50	$B_2A_2BA_{21}B_3ABA_3B_2A_2BA_{11}$
55	$BA_{15}B_4ABABA_2BAB_{11}A_{16}$
60	$BA_{10}B_3ABABA_2B_2A_2B_3A_3B_7A_3BA_{17}BA$
65	$B_2A_2BA_5BABA_8B_3A_4BA_3BA_4B_{13}A_3B_2A_{10}$
70	$B_2A_2BA_{12}B_2AB_4AB_2AB_4A_6B_6A_2BAB_2A_5B_3A_4BA_5BA$
75	$A_2BA_7BA_3BA_{10}B_{15}ABA_7B_6A_3BA_3BA_4BA_7$
80	$A_7B_2A_3BA_8B_6ABA_2B_4AB_3AB_6A_2BA_2BAB_6AB_3A_3BA_{11}B_2$
85	$B_8A_{11}B_2AB_3ABA_6B_2A_3BA_2B_5A_2B_6AB_2A_2BA_2B_2A_2BA_4B_2A_9B_2A$
90	$BABA_7BA_2B_2ABA_5BA_8BAB_6A_2B_3AB_2A_2BA_4BA_3B_2A_3BAB_6A_3BA_3B_2A_9B$
95	$A_9B_2A_8BA_3B_2ABABABA_2BAB_7AB_4ABA_3BA_4BA_2B_3A_5B_2AB_2AB_2AB_3A_{15}$
100	$B_4ABA_3BA_3B_5AB_2A_3BA_6BABA_5BA_3BA_2BAB_2ABA_2BABA_2BAB_{12}ABA_8BA_{16}$

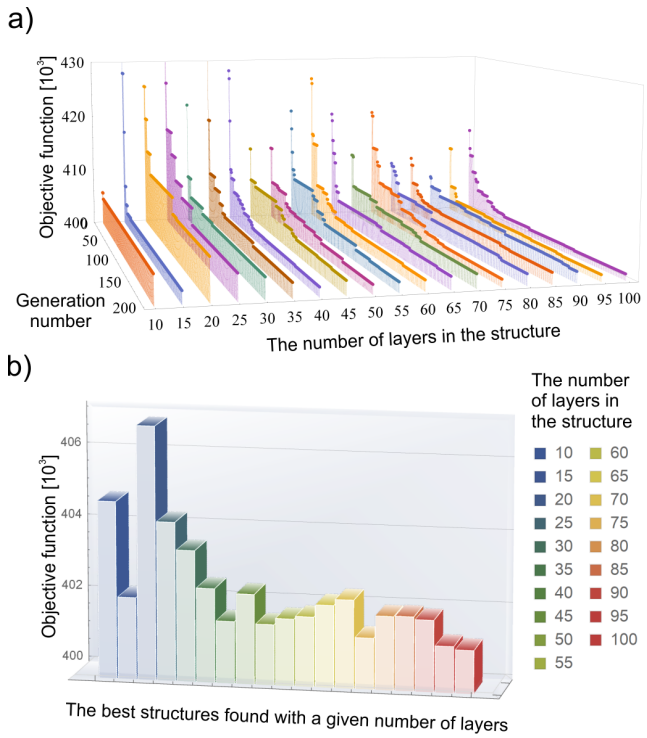

Fig. 4. The objective function values of the best individuals for each generation and the number of layers: (a) and the objective function values for the best found structures with given number of layers (b) GACL algorithm

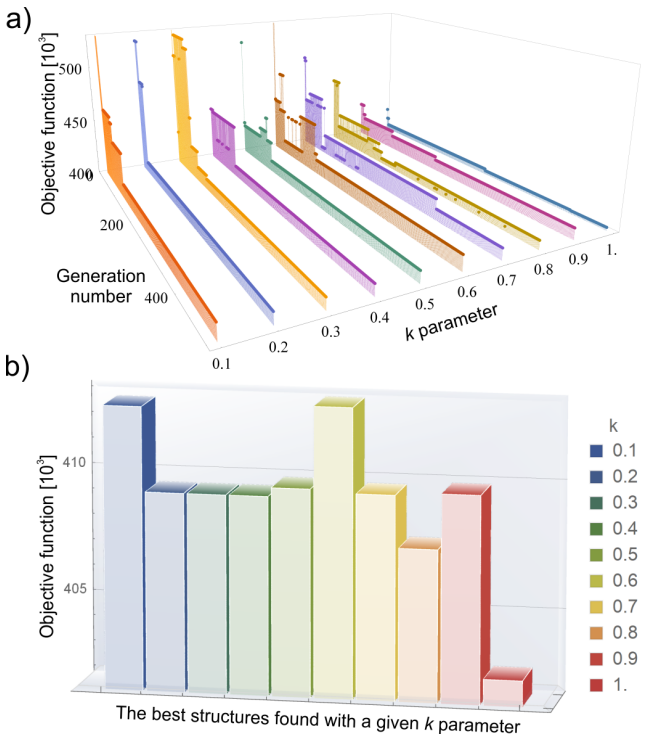

Fig. 5. The objective function values of the best individuals for each generation and the number of layers: (a) and the objective function values VOLUMEXX,2021 for the best-found structures with given number of layers (b) GAVL algorithm

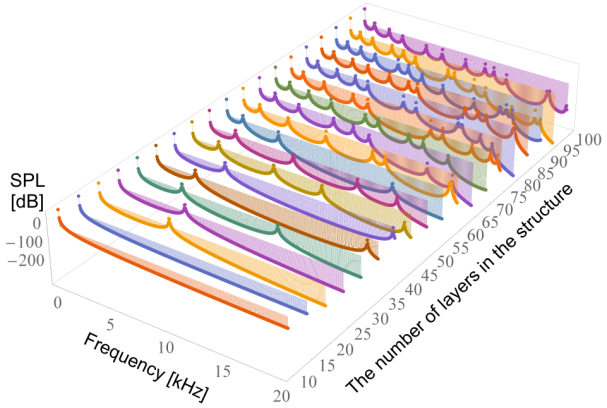

Fig. 6. Sound pressure level (SPL) in the range of acoustic frequencies for the best designated structures in GACL algorithm

value of 90 dB (the sound pressure of the source was $p_s = 0.6325$ Pa), p is transmitted wave pressure and the reference pressure is $p_0 = 2 \cdot 10^{-5}$ Pa) according to the relationship

$$SPL = 10 \log \frac{\langle p \rangle^2}{p_0^2}. \tag{15}$$

The number of possible analyzed structures (solution space) in the algorithm with a variable number of layers was $\sum_{i=10}^{100} 2^i$.

Due to the much larger space of solutions, the number of iterations of the algorithm with a variable number of layers in the structure was set to 500.

Figure 7 shows the SPL charts for the most favorable structures determined by the GACL algorithm and Table 3 shows the corresponding values of the functions F_T, F_{DI} and F_c' for the best structures in the GACL algorithm. SPL as a function of frequency for the best structures obtained with GAVL is shown in Fig. 8, and Table 4 shows the best structures obtained with the GAVL algorithm.

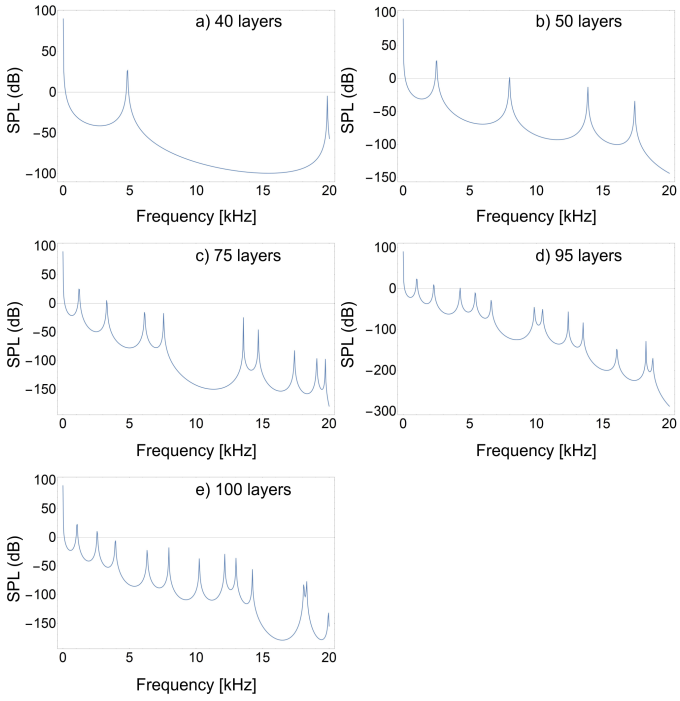

Fig. 7. Sound pressure level (SPL) in the range of acoustic frequencies for the best-designated structures in GACL algorithm

Table 3

The objective function and its components for the best-designated structures by the GACL algorithm

Number of layers	F_c'	F_T [10^{-3}]	F_{DI}
100	401 045	5.00538	4006.14
95	401 133	5.00586	4006.63
75	401 266	5.00609	4007.77
50	401 521	5.00710	4009.52
40	401 564	5.00695	4010.07

Table 4

The objective function, structures, and its components for the best-designated structures by GAVL algorithm

k	Structure	Number of layers	F_c'	F_T [10^{-3}]	F_{DI}
0.1	B_4A_6	10	412 772	5.0	4127.73
0.2	BA_7B_2	10	409 488	5.0	4094.88
0.3	B_2A_7B	10	409 488	5.0	4094.88
0.4	A_7B_3	10	409 489	5.0	4094.89
0.5	$BABA_6B$	10	409 832	5.00049	4097.92
0.6	$BABA_5B_2$	10	412 998	5.00016	4129.85
0.7	ABA_6B_2	10	409 714	5.00021	4096.97
0.8	ABA_7B	10	407 689	5.00067	4076.35
0.9	$BABA_6B$	10	409 832	5.00049	4097.92
1	$A_{13}B_4$	17	402 782	5.0	4027.82

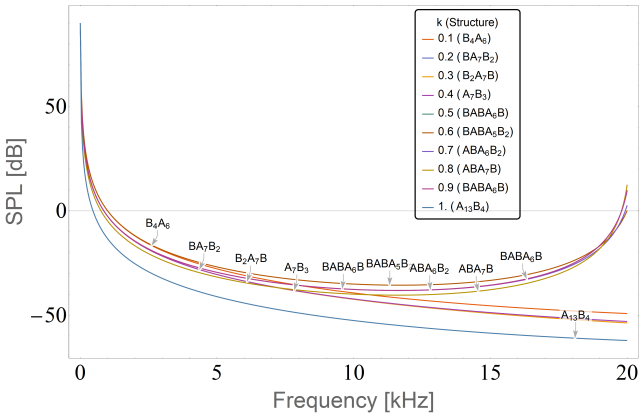

Fig. 8. Sound pressure level (SPL) in the range of acoustic frequencies for the best designated structures in GAVL algorithm

In the 40-layer structure, in the analyzed frequency range of mechanical waves up to 20 kHz, there was a single transmission peak for 4.819 kHz with an SPL value of 27 dB (Fig. 7a). In

the structures shown in Figs. 7b–e there were two transmission peaks for the number of layers, respectively: 50–2.512 kHz (27.2 dB) and 8.001 kHz (2.1 dB), 75–1.219 kHz (25.2 dB) and 3.286 kHz (5.2 dB), 95–1.029 kHz (23.8 dB) and 2.298 kHz (10.3 dB), 100–1.066 kHz (22.9 dB) and 2.584 kHz (10.5 dB). On the other hand, in the structure obtained with the use of the genetic algorithm with a variable number of layers GAVL (Fig. 8), there were no transmission peaks in the band gaps. In none of the structures, the SPL value for the occurring transmission peaks exceeded 30 dB. The values of the F_T function for all found structures are similar, and the band gap is in almost the entire range of acoustic frequencies.

4. CONCLUSIONS

The aim of the work was to minimize the transmission and the number of layers in quasi-one-dimensional phononic structures in the range of acoustic frequencies. During the research, two types of genetic algorithms were compared, differing in the objective and the crossover functions. For all the obtained optimal structures, the transmission was significantly reduced, although there were narrow transmission peaks inside the band gaps with intensity below 30 dB for the wave source at the level of 90 dB for the GACL algorithm. The transmission peaks occurred at different frequencies, so a structure suited to the application should be selected. Importantly, the designated band gaps were caused only by the structure topology. The positive extinction coefficient of lossy materials will further reduce the transmission, but its nature will not change. An additional band-pass filter in front of the structure would eliminate the occurring transmission peaks. However, the structures that were obtained by the GAVL algorithm had a wide band gap and no high-transmission peaks with a low half-width.

Almost all structures obtained as part of GAVL work had a minimum number of layers equal to 10. There were slight differences in transmission, but they were negligible as they were below the assumed limit for the band gap. The structure obtained for $k = 1$ had the most favorable transmission structure but also consisted of a larger number of layers. Based on the research, it can be concluded that the developed GAVL algorithm with an appropriately selected objective function achieved optimal solutions in a much smaller number of iterations than the GACL algorithm, and the value of the k parameter below 1 leads to faster achievement of the optimal structure.

ACKNOWLEDGEMENTS

The study has been carried out within statutory research of the Department of Mechanics and Machine Design Fundamentals of Czestochowa University of Technology.

REFERENCES

[1] Y. Pennec, B. Djafari-Rouhani, H. Larabi, J. Vasseur, and A.-C. Hladky-Hennion, "Phononic crystals and manipulation of sound", *Phys. Status Solidi C*, vol. 6, no. 9, pp. 2080–2085, Sep. 2009, doi: 10.1002/pssc.200881760.

[2] Y.F. Li, F. Meng, S. Li, B. Jia, S. Zhou, and X. Huang, "Designing broad phononic band gaps for in-plane modes", *Phys. Lett. A*, vol. 382, no. 10, pp. 679–684, Mar. 2018, doi: 10.1016/j.physleta.2017.12.050.

[3] W. Elmadih, W.P. Syam, I. Maskery, D. Chronopoulos, and R. Leach, "Multidimensional Phononic Bandgaps in Three-Dimensional Lattices for Additive Manufacturing", *Materials*, vol. 12, no. 11, p. 1878, Jun. 2019, doi: 10.3390/ma12111878.

[4] S. Garus and W. Sochacki, "High-performance quasi one-dimensional mirrors of mechanical waves built of periodic and aperiodic structures", *J. Appl. Math. Comput. Mech.*, vol. 17, no. 4, pp. 19–24, Dec. 2018, doi: 10.17512/jamcm.2018.4.03.

[5] Z. Zhang, X.K. Han, and G.M. Ji, "Mechanism for controlling the band gap and the flat band in three-component phononic crystals", *J. Phys. Chem. Solids*, vol. 123, pp. 235–241, Dec. 2018, doi: 10.1016/j.jpcs.2018.08.012.

[6] Y. Sun *et al.*, "Band gap and experimental study in phononic crystals with super-cell structure", *Results Phys.*, vol. 13, p. 102200, Jun. 2019, doi: 10.1016/j.rinp.2019.102200.

[7] A.H. Safavi-Naeini, J.T. Hill, S. Meenehan, J. Chan, S. Gröblacher, and O. Painter, "Two-Dimensional Phononic-Photonic Band Gap Optomechanical Crystal Cavity", *Phys. Rev. Lett.*, vol. 112, no. 15, p. 153603, Apr. 2014, doi: 10.1103/PhysRevLett.112.153603.

[8] W. Sochacki, "Transmission Properties of Phononical Dodecagonal Filter", *Acta Phys. Pol. A*, vol. 138, no. 2, pp. 328–331, Aug. 2020, doi: 10.12693/APhysPolA.138.328.

[9] H. Fan, B. Xia, L. Tong, S. Zheng, and D. Yu, "Elastic Higher-Order Topological Insulator with Topologically Protected Corner States", *Phys. Rev. Lett.*, vol. 122, no. 20, p. 204301, May 2019, doi: 10.1103/PhysRevLett.122.204301.

[10] M. P. Bendsøe and O. Sigmund, *Topology Optimization*. Berlin, Heidelberg: Springer Berlin Heidelberg, 2004.

[11] O. Sigmund and J. Søndergaard Jensen, "Systematic design of phononic band–gap materials and structures by topology optimization", *Philos. Trans. R. Soc. London, Ser. A*, vol. 361, no. 1806, pp. 1001–1019, May 2003, doi: 10.1098/rsta.2003.1177.

[12] L. Xie, B. Xia, J. Liu, G. Huang, and J. Lei, "An improved fast plane wave expansion method for topology optimization of phononic crystals", *Int. J. Mech. Sci.*, vol. 120, pp. 171–181, Jan. 2017, doi: 10.1016/j.ijmecsci.2016.11.023.

[13] Zhong Hui-Lin, Wu Fu-Gen, and Yao Li-Ning, "Application of genetic algorithm in optimization of band gap of two-dimensional phononic crystals", *Acta. Phys. Sin.*, vol. 55, no. 1, p. 275, 2006, doi: 10.7498/aps.55.275

[14] Z. Liu, B. Wu, and C. He, "Band-gap optimization of two-dimensional phononic crystals based on genetic algorithm and FPWE", *Waves Random Complex Media*, vol. 24, no. 3, pp. 286–305, Jul. 2014, doi: 10.1080/17455030. 2014.901582.

[15] X. Huang and Y.M. Xie, "Bi-directional evolutionary topology optimization of continuum structures with one or multiple materials", *Comput. Mech.*, vol. 43, no. 3, pp. 393–401, Feb. 2009, doi: 10.1007/s00466-008-0312-0.

[16] H.-W. Dong, X.-X. Su, Y.-S. Wang, and C. Zhang, "Topological optimization of two-dimensional phononic crystals based on the finite element method and genetic algorithm", *Struct. Multidisc. Optim.*, vol. 50, no. 4, pp. 593–604, Oct. 2014, doi: 10.1007/s00158-014-1070-6.

[17] Y. Li, X. Huang, and S. Zhou, "Topological Design of Cellular Phononic Band Gap Crystals", *Materials*, vol. 9, no. 3, p. 186, Mar. 2016, doi: 10.3390/ma9030186.

[18] G.A. Gazonas, D.S. Weile, R. Wildman, and A. Mohan, "Genetic algorithm optimization of phononic bandgap structures", *Int. J. Solids Struct.*, vol. 43, no. 18–19, pp. 5851–5866, Sep. 2006, doi: 10.1016/j.ijsolstr.2005. 12.002.

[19] M.I. Hussein, K. Hamza, G.M. Hulbert, R.A. Scott, and K. Saitou, "Multiobjective evolutionary optimization of periodic layered materials for desired wave dispersion characteristics", *Struct. Multidisc. Optim.*, vol. 31, no. 1, pp. 60–75, Jan. 2006, doi: 10.1007/s00158-005-0555-8.

[20] K.L. Manktelow, M.J. Leamy, and M. Ruzzene, "Topology design and optimization of nonlinear periodic materials", *J. Mech. Phys. Solids*, vol. 61, no. 12, pp. 2433–2453, Dec. 2013, doi: 10.1016/j.jmps.2013.07.009.

[21] S. Hedayatrasa, M. Kersemans, K. Abhary, M. Uddin, J.K. Guest, and W. Van Paepegem, "Maximizing bandgap width and in-plane stiffness of porous phononic plates for tailoring flexural guided waves: Topology optimization and experimental validation", *Mech. Mater.*, vol. 105, pp. 188–203, Feb. 2017, doi: 10.1016/j.mechmat.2016.12.003.

[22] L. Chen, Y. Guo, and H. Yi, "Optimization study of bandgaps properties for two-dimensional chiral phononic crystals base on lightweight design", *Phys. Lett. A*, vol. 388, p. 127054, Feb. 2021, doi: 10.1016/j.physleta.2020.127054.

[23] X.K. Han and Z. Zhang, "Bandgap design of three-phase phononic crystal by topological optimization", *Wave Motion*, vol. 93, p. 102496, Mar. 2020, doi: 10.1016/j.wavemoti.2019.102496.

[24] S. Garus and W. Sochacki, "Structure optimization of quasi one-dimensional acoustic filters with the use of a genetic algorithm", *Wave Motion*, vol. 98, p. 102645, Nov. 2020, doi: 10.1016/j.wavemoti.2020.102645.

[25] Y. Chen, F. Meng, G. Sun, G. Li, and X. Huang, "Topological design of phononic crystals for unidirectional acoustic transmission", *J. Sound Vib.*, vol. 410, pp. 103–123, Dec. 2017, doi: 10.1016/j.jsv.2017.08.015.

[26] X.K. Han and Z. Zhang, "Topological Optimization of Phononic Crystal Thin Plate by a Genetic Algorithm", *Sci. Rep.*, vol. 9, no. 1, p. 8331, Dec. 2019, doi: 10.1038/s41598-019-44850-8.

[27] Ł. Chruszczyk, "Genetic minimisation of peak-to-peak level of a complex multi-tone signal", *Bull. Pol. Acad. Sci. Tech. Sci.*, vol. 67, no. 3, pp. 621–629, 2019, doi: 10.24425/BPASTS.2019.129660.

[28] M. Beniyel, M. Sivapragash, S.C. Vettivel, P. Senthil Kumar, K.K. Ajith Kumar, and K. Niranjan, "Optimization of tribology parameters of AZ91D magnesium alloy in dry sliding condition using response surface methodology and genetic algorithm", *Bull. Pol. Acad. Sci. Tech. Sci.*, vol. 69, no. 1, p. e135835, 2021, doi: 10.24425/BPASTS.2021.135835.

[29] O. Dazel, J.-P. Groby, B. Brouard, and C. Potel, "A stable method to model the acoustic response of multilayered structures", *J. Appl. Phys.*, vol. 113, no. 8, p. 083506, Feb. 2013, doi: 10.1063/1.4790629.

[30] S. Garus, W. Sochacki, and M. Bold, "Comparison of phononic structures with piezoelectric $0.62Pb(Mg_{1/3}Nb_{1/3})O_3$-$0.38PbTiO_3$ defect layers", in *Proc. Engineering Mechanics 2018*, Svratka, Czech Republic, May 2018, pp. 229–232, doi: 10.21495/ 91-8-229.

[31] M.M. Sigalas and C.M. Soukoulis, "Elastic-wave propagation through disordered and/or absorptive layered systems", *Phys. Rev. B*, vol. 51, no. 5, pp. 2780–2789, Feb. 1995, doi: 10.1103/PhysRevB.51.2780.

[32] P.-G. Luan and Z. Ye, "Acoustic wave propagation in a one-dimensional layered system", *Phys. Rev. E*, vol. 63, no. 6, p. 066611, May 2001, doi: 10.1103/PhysRevE.63.066611.

[33] M.-I. Pop and N. Cretu, "Intrinsic transfer matrix method and split quaternion formalism for multilayer media", *Wave Motion*, vol. 65, pp. 105–111, Sep. 2016, doi: 10.1016/j.wavemoti.2016.04.011.

[34] S. Yang, W.-D. Yu, and N. Pan, "Band structure in two-dimensional fiber–air photonic crystals", *Physica B*, vol. 406, no. 4, pp. 963–966, Feb. 2011, doi: 10.1016/j.physb.2010.12.039.

[35] M. Fukuhara, X. Wang, and A. Inoue, "Acoustic analysis of the amorphous phase of annealed Zr55Cu30Ni5Al10 glassy alloy, using diffracted SH ultrasonic waves", *J. Non-Cryst. Solids*, vol. 356, no. 33–34, pp. 1707–1710, Jul. 2010, doi: 10.1016/j.jnoncrysol.2010.06.025.